Investigation of Tropical Rain Cells with ERS SAR Imagery and Ground-Based Weather Radar

Dayalan Kasilingam, I-I Lin, Hock Lim, Victor Khoo
Centre for Remote Imaging, Sensing and Processing (CRISP), Faculty of Science, National University of Singapore, Lower Kent Ridge Road, Singapore 119260
Tel: 65-7723220 Fax: 65-7757717
Email: crsdpk nus.sg, crslinii nus.sg

Werner Alpers
Institute of Oceanography, University of Hamburg, Troplowitzstr. 7, D-22529 Hamburg
Tel: 040-41235432 Fax: 040-41235713
Email: alpers ifm.uni-hamburg.de

Tian Kuay Lim
Meteorological Service Singapore, P.O. Box 8, Changi Airport Post Office,
Singapore Changi Airport, Singapore 918141
Tel: 65-5422863 Fax: 65-5425026
Email: mssltk pacific.net.sg

ABSTRACT

ERS-1/2 SAR images acquired over ocean areas showing radar signatures of four different kinds of tropical rain cells, ordinary storm cells, supercell storms, multicell storms, and squall lines, are presented. One ERS-2 SAR image showing radar signature of a squall line south of Singapore is compared with simultaneously acquired ground-based weather radar data. Matching of features in the SAR and weather radar data helped locating of the gust front and the area of updraft convergence, and suggested an explanation of the mottled structure associated with the rain band. It is also shown that the area of heavy rain (> 50 mm/hr) is associated with a reduction of backscattered radar power, which is likely due to attenuation by rain drops in the atmosphere.

1. INTRODUCTION

Tropical rain cells consist of convective clouds (cumulonimbus clouds or thunderstorms) which are the source of heavy rainfall and lightning in the equatorial regions (Ray, 1986; Cotton and Anthes, 1989). Ever since the SEASAT mission in 1978, storm footprints on the sea surface have been reported regularly in SAR images (Fu and Holt, 1982; Atlas, 1994a; Atlas, 1994b; Atlas and Black, 1994, Iguchi, 1995; Lichtenegger, 1996, Melsheimer et al., 1996). Investigation of these footprints has been hindered by the lack of in situ measurements. To a large extent, the interpretation still remains speculative. Though the potential of using ground or ship-based weather radar data for comparison has long been recognised, only a few cases of collocated data sets are available. Atlas (1994b), Atlas and Black (1994), and Iguchi et al (1995) are some of the very few studies on radar signatures of rain cells in which weather radar data has been incorporated.

SAR images from the ERS-1/2 satellites acquired by the Centre for Remote Imaging, Sensing and Processing (CRISP) ground station in Singapore, often show radar signatures of rain cells. Between 1995-1996 more than 50 clear rain cell scenes were acquired. Among the 50 scenes, several SAR scenes are collocated with weather radar data sets from the Meteorological Service Singapore. In this paper, we present SAR images showing radar signatures of four types of rain cells. In particular, a detailed analysis is performed on one scene containing a squall line. This SAR scene is compared with the weather radar data to analyse and identify its salient characteristics.

2. TROPICAL RAIN CELLS

In meteorology, rain cells are categorised into four different groups - ordinary storm cells, supercell storms, multicell storms, and squall lines (Ray, 1986; Cotton and Anthes, 1989). Ordinary storms are cumulonimbus clouds which undergo three stages of evolution: the cumulus, the mature, and the dissipating stage. During the cumulus stage, cloud towers are formed which are associated with updrafts. In the mature stage, cumulus elements of the cloud towers merge into a larger scale convective system. Downdrafts, rainfall and gust fronts are the major characteristics (figure 1). Downdrafts, diminishing convective rainfall, and prevailing stratiform precipitation are observed at the dissipating stage. Supercell storms differ from ordinary storms by their size, intensity, and time span. Multicell storms usually consist of two to four cells, while squall lines consist of clusters of rain cells which are organised in lines and whose physical dimension can be of the order of hundreds of kilometres. ERS SAR scenes which appears to show the above mentioned types of rain cells acquired by CRISP are shown in figures 2-5. The signature of the rain cell in the SAR images may be due to three distinct physical processes. First there is the contribution due to the rain column in the atmosphere. In some SAR images, the attenuation due to the rain column may diminish the radar return from the ocean surface. In addition, there may be a contribution due to scattering from the rain. Next there is the effect of rain impinging on the sea surface. This may perturb the surface sufficiently to change the characteristics of backscattered signal. Finally there is the impact of the downdraft associated with the rainfall on the sea surface roughness. This increased near surface wind due to the downdraft will modulate sea surface roughness thus the backscattered signal. Most of the raincell signatures seen in the ERS SAR images are due to a combination of these three processes (Melsheimer et al, 1996).

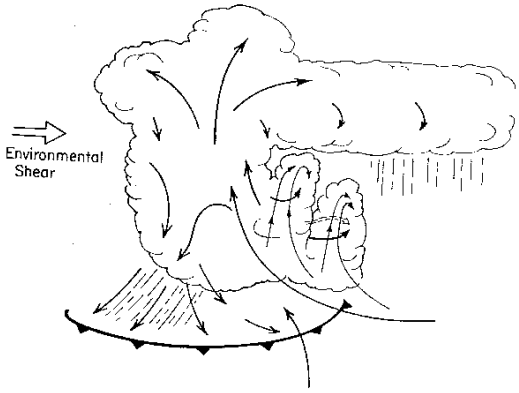

Figure 1: Schematic illustration of an ordinary storm cell at its mature stage (from Cotton and Anthes, 1989).

Figure 2: ERS-2 SAR image of an ordinary storm over the Andaman sea acquired on April 5, 1996, at 04.04 UTC.

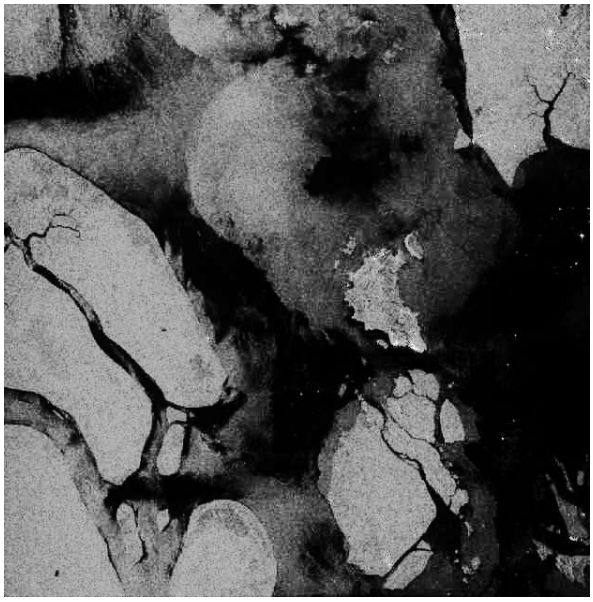

Figure 3: ERS-1 SAR image of a possible supercell storm near Singapore acquired on April 28, 1996, at 15.47 UTC.

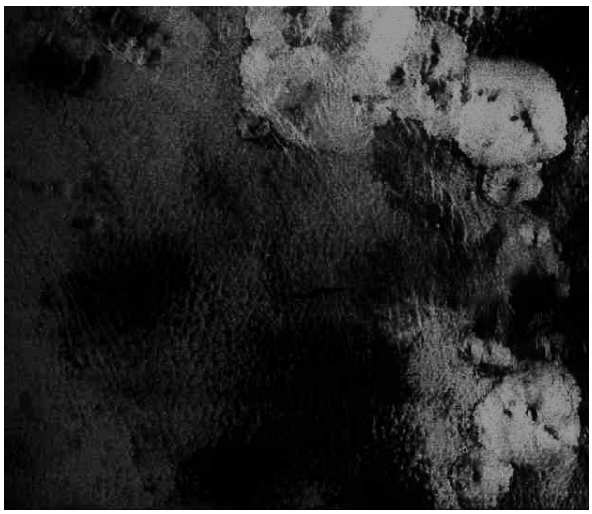

Figure 4: ERS-1 SAR image of a multicell storm over the Andaman sea acquired on April 4, 1996, at 04.05 UTC.

3. GROUND-BASED WEATHER RADAR

Data from the two S-band (10 cm wavelength) ground-based weather radars at Singapore is used to validate the analysis of the SAR scenes. Two types of weather radar data sets are used.

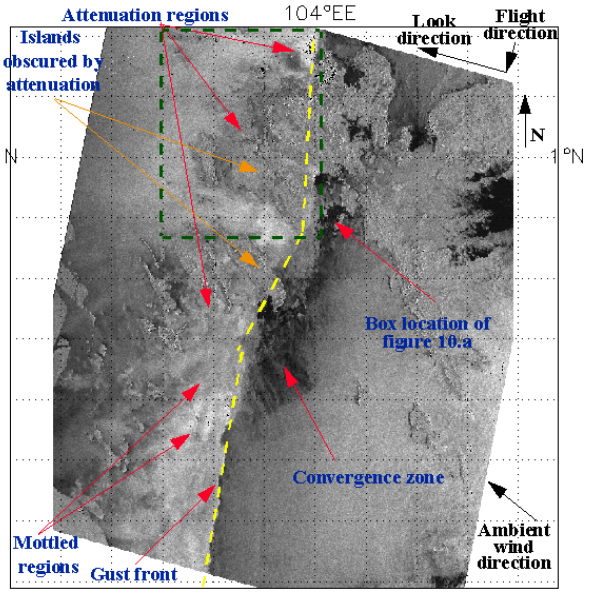

Figure 5: ERS-2 SAR imagery of a squall line at the coast of Singapore acquired on September 22, 1996, at 03.24 UTC. For comparison with weather radar data, this image is displayed on a equidistant cylindrical map projection.

The first type is the digital radar image. Digital data within a 60 km radius centred in Singapore was recorded. Reflectivity information which is a measure of the backscattered radar power from rain, is obtained every 5 minutes. Six levels of reflectivity are available. The corresponding rainfall rates vary from less than 0.25 mm/hr to more than 125 mm/hr. These rates are derived from the Z-R relationship given by $Z = 200R^{1.6}$, where *Z* and *R* are the reflectivity factor and the rainfall rate (mm/hr), respectively. For the squall line event on 22nd September 1996, the entire range of 6 levels is found (figure 6). Taken 1 minute (03.25 UTC) after the SAR acquisition (03.24 UTC), this image is best suited for interpreting the SAR signature of a squall line.

The other type of radar data is the hourly hand-plotted records of the PPI display . The recorded data range is 400 km. This analogue data set complements the digital data set, since the complete structure of the squall line can be observed. Figures 7 and 8 show analogue weather radar plots which were acquired on September 22, 1996, at 03.00 UTC and 04.00 UTC. These two images show the evolution and movement of the squall line before and after the SAR data acquisition.

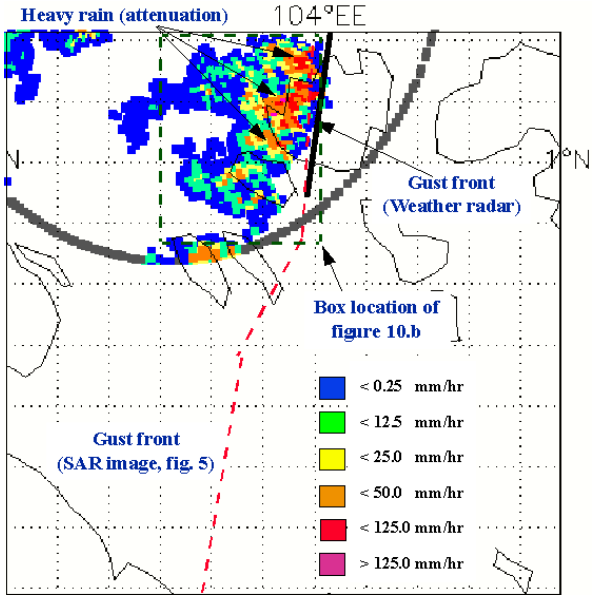

Figure 6: Simultaneous measurements from the digital weather radar of the squall line seen in figure 5. This image was taken at 03.25 UTC, i.e., 1 minute after the SAR acquisition. The effective range of the weather radar is shown by the circular line inserted in the image.

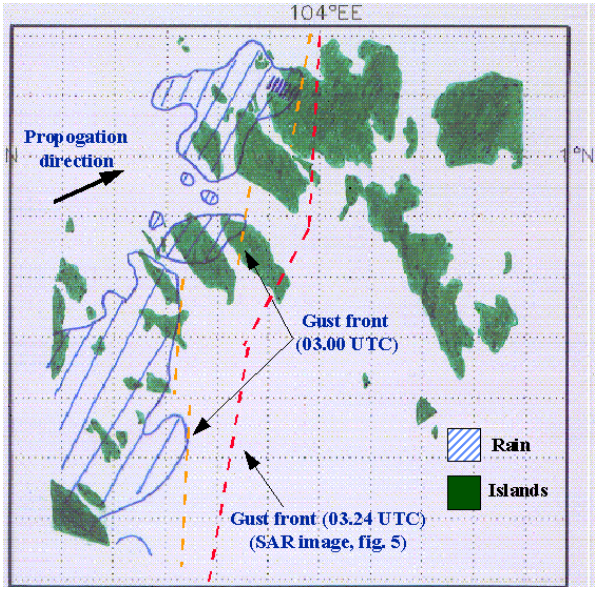

Figure 7: Collocated plot from the hourly PPI display of the squall line event of September 22, 1996. This plot was taken at 03.00 UTC, 24 minutes before the acquisition of the SAR scene (figure 5) at the same location. The hashed region corresponds to high radar reflectivity associated with the rain band. Features including rain band and gust front match well with the SAR scene. It can be seen clearly that the squall line has moved towards north east during the 24 minutes between weather radar and SAR data acquisition.

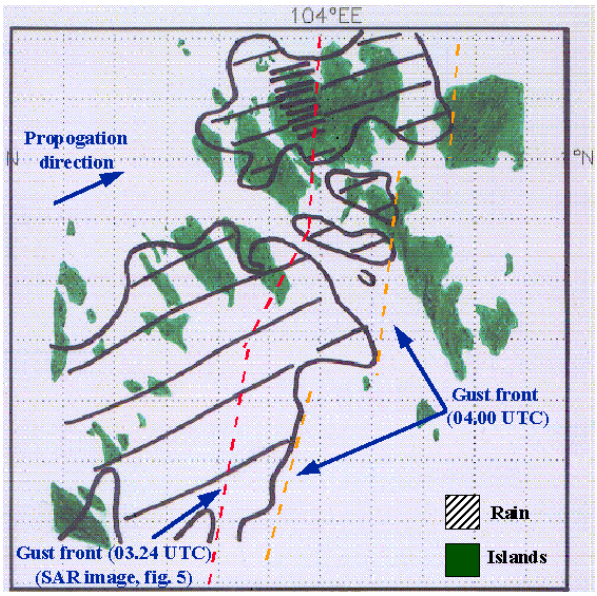

Figure 8: Collocated plot from the hourly PPI display of the squall line event of September 22, 1996. This plot was taken at 04.00 UTC, i.e., 36 minutes after the acquisition of the SAR scene (figure 5) at the same location. The squall line continued to move north-eastwards and the rain band has expanded.

4. COMPARISON BETWEEN ERS SAR SCENE AND WEATHER RADAR DATA

Hourly radar plots (figures 7-8) are first used to confirm the existence of the squall line. At 03.00 UTC (figure 7), the rain band containing linearly aligned cells stretching vertically across the plot is clearly observed. The gust front can thus be delineated. Since the gust front is the interface between cold downdraft and warm ambient air, it is always located at the forefront of the cells. Therefore, rain bands exist only at the rear (left) side of the gust front, whereas no rain is encountered at the forefront. At 04.00 UTC (figure 8), the rain band has expanded and has moved north-eastwards. The SAR scene (figure 5) was taken at 03.24 UTC, i.e., at a time between these two weather radar plots acquisitions. The gust front of the squall line can also be identified in the SAR scene corresponding to the sharp boundary running vertically across the scene. This boundary has the same orientation as the gust front visible in the two weather radar plots (figures 7 and 8) and its location is also in between them. Further evidence is provided by comparing the SAR scene with the simultaneously acquired digital weather radar image (figure 6) as the 2 boundaries match nearly exactly.

In figure 6, we can see a region of high reflectivity corresponding to a high rainfall rate (> 50 mm/hr). This region matches well with the dark feature visible in the SAR scene. As the dark feature covers both land and sea, we interpret this as an indication that the radar backscatter is reduced by the attenuation of the rain column in the atmosphere. It is unlikely that it is caused by rain impinging on the sea surface or by wind effects, because the pootprints has been hindered by the lack of in situ measurements. To a large extent, the interpretation still remains speculative. Though the potential of using ground or ship-based weather radar data for comparison has long been recognised, only a few cases of collocated data sets are available. Atlas (1994b), Atlas and Black (1994), and Iguchi et al (1995) are some of the very few studies on radar signatures of rain cells in which weather radar data has been incorporated.

SAR images from the ERS-1/2 satellites acquired by the Centre for Remote Imaging, Sensing and Processing (CRISP) ground station in Singapore, often show radar signatures of rain cells. Between 1995-1996 more than 50 clear rain cell scenes were acquired. Among the 50 scenes, several SAR scenes are collocated with weather radar data sets from the Meteorological Service Singapore. In this paper, we present SAR images showing radar signatures of four types of rain cells. In particular, a detailed analysis is performed on one scene containing a squall line. This SAR scene is compared with the weather radar data to analyse and identify its salient characteristics.

2. TROPICAL RAIN CELLS

In meteorology, rain cells are categorised into four different groups - ordinary storm cells, supercell storms, multicell storms, and squall lines (Ray, 1986; Cotton and Anthes, 1989). Ordinary storms are cumulonimbus clouds which undergo three stages of evolution: the cumulus, the mature, and the dissipating stage. During the cumulus stage, cloud towers are formed which are associated with updrafts. In the mature stage, cumulus elements of the cloud towers merge into a larger scale convective system. Downdrafts, rainfall and gust fronts are the major characteristics (figure 1). Downdrafts, diminishing convective rainfall, and prevailing stratiform precipitation are observed at the dissipating stage. Supercell storms differ from ordinary storms by their size, intensity, and time span. Multicell storms usually consist of two to four cells, while squall lines consist of clusters of rain cells which are organised in lines and whose physical dimension can be of the order of hundreds of kilometres. ERS SAR scenes which appears to show the above mentioned types of rain cells acquired by CRISP are shown in figures 2-5. The signature of the rain cell in the SAR images may be due to three distinct physical processes. First there is the contribution due to the rain column in the atmosphere. In some SAR images, the attenuation due to the rain column may diminish the radar return from the ocean surface. In addition, there may be a contribution due to scattering from the rain. Next there is the effect of rain impinging on the sea surface. This may perturb the surface sufficiently to change the characteristics of backscattered signal. Finally there is the impact of the downdraft associated with the rainfall on the sea surface roughness. This increased near surface wind due to the downdraft will modulate sea surface roughness thus the backscattered signal. Most of the raincell signatures seen in the ERS SAR images are due to a combination of these three processes (Melsheimer et al, 1996).

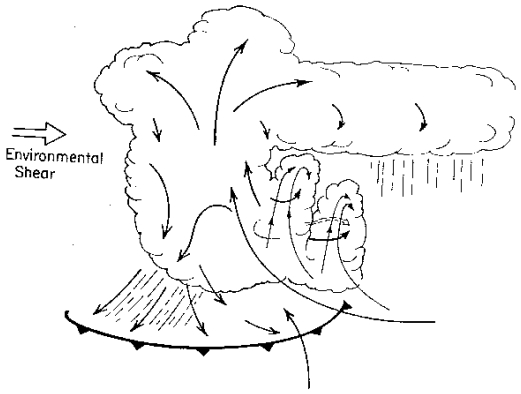

Figure 1: Schematic illustration of an ordinary storm cell at its mature stage (from Cotton and Anthes, 1989).

Figure 2: ERS-2 SAR image of an ordinary storm over the Andaman sea acquired on April 5, 1996, at 04.04 UTC.

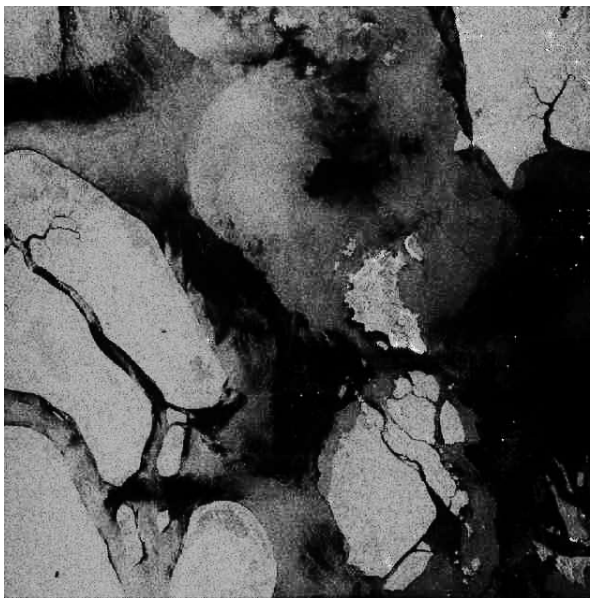

Figure 3: ERS-1 SAR image of a possible supercell storm near Singapore acquired on April 28, 1996, at 15.47 UTC.

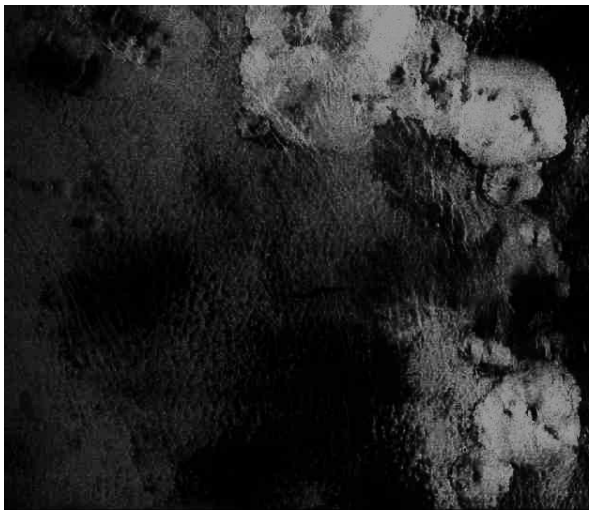

Figure 4: ERS-1 SAR image of a multicell storm over the Andaman sea acquired on April 4, 1996, at 04.05 UTC.

3. GROUND-BASED WEATHER RADAR

Data from the two S-band (10 cm wavelength) ground-based weather radars at Singapore is used to validate the analysis of the SAR scenes. Two types of weather radar data sets are used.

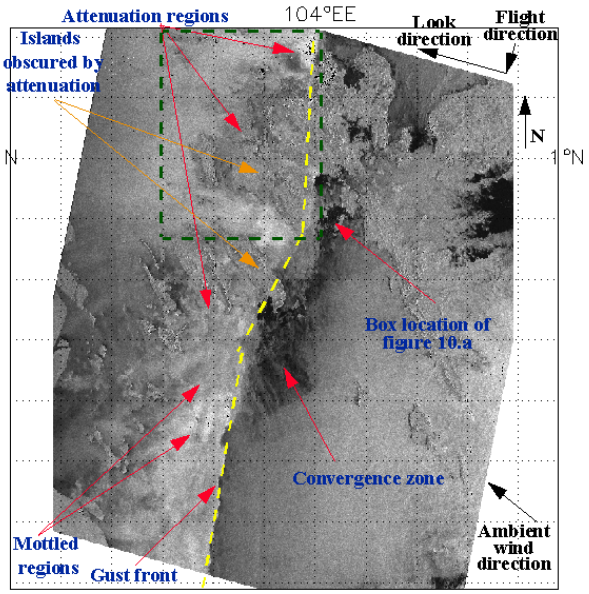

Figure 5: ERS-2 SAR imagery of a squall line at the coast of Singapore acquired on September 22, 1996, at 03.24 UTC. For comparison with weather radar data, this image is displayed on a equidistant cylindrical map projection.

The first type is the digital radar image. Digital data within a 60 km radius centred in Singapore was recorded. Reflectivity information which is a measure of the backscattered radar power from rain, is obtained every 5 minutes. Six levels of reflectivity are available. The corresponding rainfall rates vary from less than 0.25 mm/hr to more than 125 mm/hr. These rates are derived from the Z-R relationship given by $Z = 200R^{1.6}$, where *Z* and *R* are the reflectivity factor and the rainfall rate (mm/hr), respectively. For the squall line event on 22nd September 1996, the entire range of 6 levels is found (figure 6). Taken 1 minute (03.25 UTC) after the SAR acquisition (03.24 UTC), this image is best suited for interpreting the SAR signature of a squall line.

The other type of radar data is the hourly hand-plotted records of the PPI display . The recorded data range is 400 km. This analogue data set complements the digital data set, since the complete structure of the squall line can be observed. Figures 7 and 8 show analogue weather radar plots which were acquired on September 22, 1996, at 03.00 UTC and 04.00 UTC. These two images show the evolution and movement of the squall line before and after the SAR data acquisition.

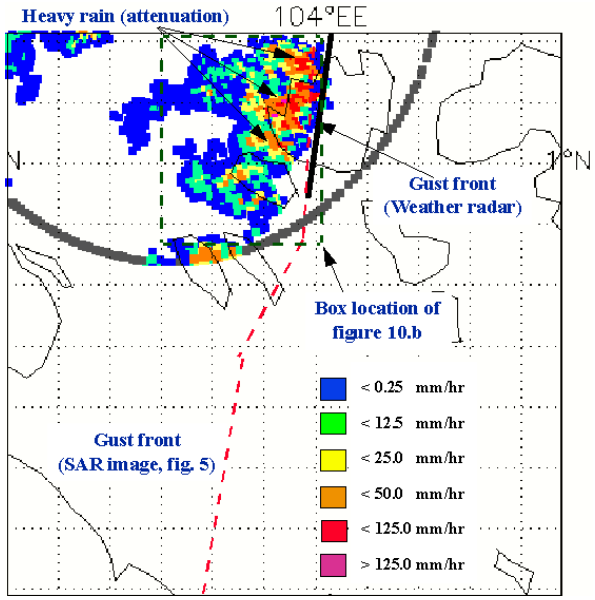

Figure 6: Simultaneous measurements from the digital weather radar of the squall line seen in figure 5. This image was taken at 03.25 UTC, i.e., 1 minute after the SAR acquisition. The effective range of the weather radar is shown by the circular line inserted in the image.

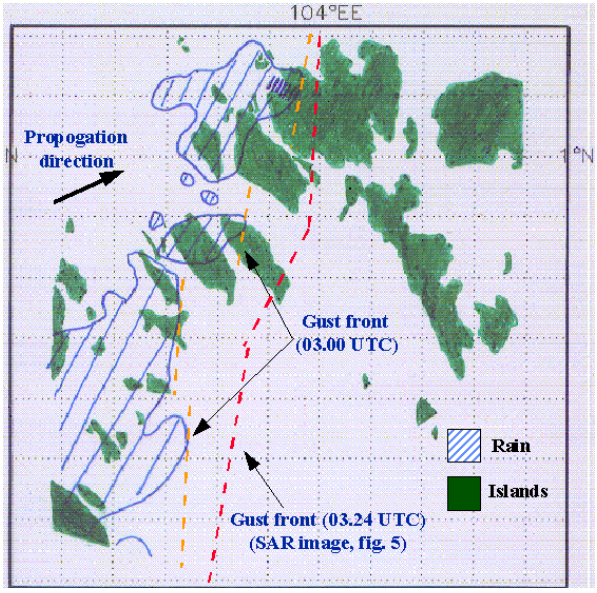

Figure 7: Collocated plot from the hourly PPI display of the squall line event of September 22, 1996. This plot was taken at 03.00 UTC, 24 minutes before the acquisition of the SAR scene (figure 5) at the same location. The hashed region corresponds to high radar reflectivity associated with the rain band. Features including rain band and gust front match well with the SAR scene. It can be seen clearly that the squall line has moved towards north east during the 24 minutes between weather radar and SAR data acquisition.

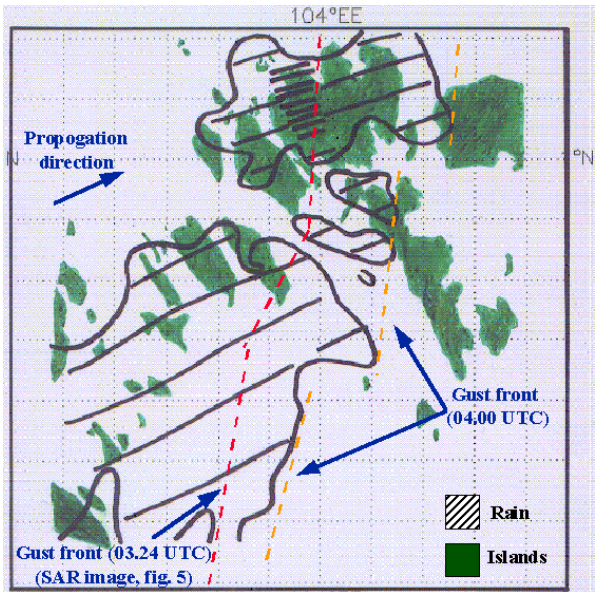

Figure 8: Collocated plot from the hourly PPI display of the squall line event of September 22, 1996. This plot was taken at 04.00 UTC, i.e., 36 minutes after the acquisition of the SAR scene (figure 5) at the same location. The squall line continued to move north-eastwards and the rain band has expanded.

4. COMPARISON BETWEEN ERS SAR SCENE AND WEATHER RADAR DATA

Hourly radar plots (figures 7-8) are first used to confirm the existence of the squall line. At 03.00 UTC (figure 7), the rain band containing linearly aligned cells stretching vertically across the plot is clearly observed. The gust front can thus be delineated. Since the gust front is the interface between cold downdraft and warm ambient air, it is always located at the forefront of the cells. Therefore, rain bands exist only